Supercapacitors from Free-Standing Polypyrrole/Graphene Nanocomposites

Citation: De Oliveira, Helinando P., Stefanie A. Sydlik, and Timothy M. Swager. "Supercapacitors from Free-Standing Polypyrrole/Graphene Nanocomposites." The Journal of Physical Chemistry C 117, no. 20 (May 23, 2013): 10270–10276.

As Published: http://dx.doi.org/10.1021/jp400344u

Publisher: American Chemical Society (ACS)

Persistent URL: http://hdl.handle.net/1721.1/86336

Version: Author's final manuscript: final author's manuscript post peer review, without publisher's formatting or copy editing

Supercapacitors from Free-Standing Polypyrrole/Graphene Nanocomposites

Journal:	*The Journal of Physical Chemistry*
Manuscript ID:	jp-2013-00344u.R2
Manuscript Type:	Article
Date Submitted by the Author:	23-Apr-2013
Complete List of Authors:	de Oliveira, Helinando; Universidade Federal do Vale do São Francisco, Materials Science Sydlik, Stefanie; Massachusetts Institute of Technology, Chemistry Swager, Timothy; Massachusetts Institute of Technology, Chemistry

Supercapacitors from Free-Standing Polypyrrole/Graphene Nanocomposites

Helinando P. de Oliveira[a,b*] *, Stefanie A. Sydlik*[a] *and Timothy M. Swager*[a*]

[a] Department of Chemistry and Institute for Soldier Nanotechnologies, Massachusetts Institute of Technology,

77 Massachusetts Avenue, Cambridge, Massachusetts 02139, United States

[b] Instituto de Pesquisa em Ciência dos Materiais, Universidade Federal do Vale do São Francisco, Juazeiro, Bahia, 48902-300, Brazil

Corresponding Author

*Timothy M. Swager (tswager@mit.edu) and Helinando P. de Oliveira (helinando.oliveira@univasf.edu.br)

ABSTRACT

Interfacial/*in situ* oxidative polymerization of polypyrrole in the presence of functionalized graphene sheets produces high-quality composites for supercapacitors, as analyzed by electrochemical impedance spectroscopy and cyclic voltammetry analysis. The synergistic interaction induced by the growth of p-type polypyrrole on the surface of negatively charged carboxylate functionalized graphene sheets results in higher storage capacity than graphene-only or polymer-only films. The high conductivity of p-doped polypyrrole and high surface area of graphene promotes high charge accumulation in capacitors. We report the optimization of the relative concentrations of carboxylate functionalized graphene in the polypyrrole matrix to maximize the composition's capacitance to 277.8 F/g.

KEYWORDS

Graphene Oxide; Polypyrrole; Supercapacitors; Electrical Impedance Spectroscopy.

INTRODUCTION

Optimal utilization of energy generated by alternative methods and associated electrical technologies (such as hybrid electric vehicles)[1] require eco-friendly high-power energy storage materials.[2,3] Supercapacitors (also known as ultracapacitors) are electrochemical structures that are characterized by high power densities and high cycle lifetimes.[4-6] The simplest supercapacitor is composed of two symmetrical electrodes that are separated by a porous substrate and an electrolyte. In this configuration, an ionic current is established between electrodes with charging and discharging.[7] In a symmetrical 2-electrode configuration, both electrodes are covered by a material of mass **m** with a specific capacitance that is four times the capacitance of cell [7] as measured from a typical discharging curve according to Eq. 1, where **dV/dt** is the slope of discharge curve at constant current **I**.

$$c_{sp}\left(\frac{F}{g}\right) = \frac{4I}{m\left(\frac{dV}{dt}\right)} \quad \text{Eq. 1}$$

Supercapacitors are typically classified as either electric double-layer capacitors (EDLC) or pseudocapacitors. In an EDLC, the capacitance arises from surface charge accumulation as a result of rapid adsorption/desorption of electrolyte ions at the electrode/electrolyte interface. This double layer has an inner layer or Helmholtz layer (closest to electrode) with charged species that are specifically adsorbed on electrode and an outer diffuse layer that extends into the bulk of solution. Ions in this latter region, which are affected by thermal agitation, are defined as nonspecifically adsorbed.[5,6,8-10]

The contribution of both terms (C_H – capacitance of the Helmholtz layer and C_{dif} – capacitance of the diffuse layer) to the total capacitance (C_T) is given by Eq. 2:

$$\frac{1}{C_T} = \frac{1}{C_H} + \frac{1}{C_{dif}} \quad \text{Eq .2}$$

Pseudocapacitors have received increasing attention as devices have greater energy storage capacity and rapid Faradic electron-transfer processes utilizing electroactive metal oxides and conducting polymers dominate their charge/discharge cycles. Optimized composites with maximum charge storage therefore include electroactive materials, high surface areas, good electrical conductivity to enable high power output, and mechanical strength to withstand the stresses associated with repeated charging/discharging cycles.[4]

Composites of conducting polymers and carbon have been reported in the literature as promising prototype materials for supercapacitor applications. Chemical synthesis of composites is preferable in comparison to electrochemical methods for consideration of large-scale production.[11] Noncovalent strategies (such as in situ polymerization) [12] are favored by good dispersability of carbon materials in water and can produce materials with improved processability, surface area and conductivity. Typically the polymerization is conducted by solution mixing of components and takes place with competitive homogeneous and heterogeneous nucleation. [12] Different arrangements of conducting polymer/carbon have been considered such as a skeleton/skin structure of SWCNT and PANI in which high conductivity is associated with flexibility.[13] Strong interactions between the conducting polymer and carbon derivatives have created single-walled carbon nanotubes/polypyrrole,[14] multi-walled carbon nanotubes/polypyrrole,[15] and core-shell polyaniline/carbon nanofibers[16] compositions with specific capacitances of 144, 190 and 264 F/g, respectively.

Graphene is a single-atom-layer two-dimensional sheet of sp^2 hexagonal carbons with outstanding electrical properties, mechanical and chemical stability, and large surface area.

The application of graphene as electrode for supercapacitors is attractive as a result of its high surface area (in order of 2630 m^2g^{-1}),[17] good mechanical stability, intrinsic mechanical strength and high electrical and thermal conductivity[18] which provides high power density. However, the stacking of graphene nanosheets represents a limitation for development of supercapacitors.[17] In order to circumvent the aggregation of graphene sheets, recent efforts have been directed on the development of hybrid carbon conductive structures such as carbon nanotube/ graphene films,[19] N- doped graphene[20] and composites of metal oxide/ graphene.[21]

Low-cost solution processable graphene compositions often begin with the production of graphene oxide (GO),[22] produced from the aggressive oxidation of graphite. GO is characterized by abundance of oxygen containing functional groups in the basal planes and edges, and as a result of the associated disruptions to the π-network, GO has a relatively low electrical conductivity. The high oxygen content in GO imparts high reactivity and it is readily reductively converted to disordered/defective graphite compositions with heating, mild reduction, or base treatment. Our group has recently developed methods to produce graphenes with robust functional groups capable of forming stable dispersions.[23a-23c] These transformations and associated reductions restore some of the electronic conductivity to the graphene sheets and the use of our Johnson-Claisen functionalization scheme produces materials (CG) with $–CH_2CO_2H$ groups on the graphene basal surface[23c] and provides for excellent dispersions in aqueous media compatible with generation of polypyrrole (PPy) to produce the nanocomposite (CG/PPy). As a result of the abundant negative charge on the CG surfaces, electrostatic forces cause strong interactions between the basal planes of the cationic PPy generated in the polymerization. [24-28]

MATERIALS AND METHODS

Ferric chloride (Pfaltz & Bauer) and 1-butyl-3-methylimidazolium hexafluorophosphate (Solvent Innovation), potassium chloride (Mallinckrodt), chloroform (VWR International), ammonium persulfate (J. T. Baker) were used as received. Pyrrole (SAFC) was distilled before each new polymerization. Graphene oxide was prepared from a modified Hummers method [29] and converted to CG (Figure 1) according to published procedures.[23c] For these purposes, graphene oxide (GO) was suspended in triethylorthoacetate, which was used as the reagent and solvent, and *para*-toluene sulfonic acid was added to catalyze the Claisen rearrangement. After the reaction was completed, ethanol with sodium hydroxide was added to encourage the formation of the carboxylate ion. (Further synthetic details can be found in the supporting information.) Nanocomposites were synthesized by two different methods (interfacial and *in situ* oxidative polymerization) as described below.

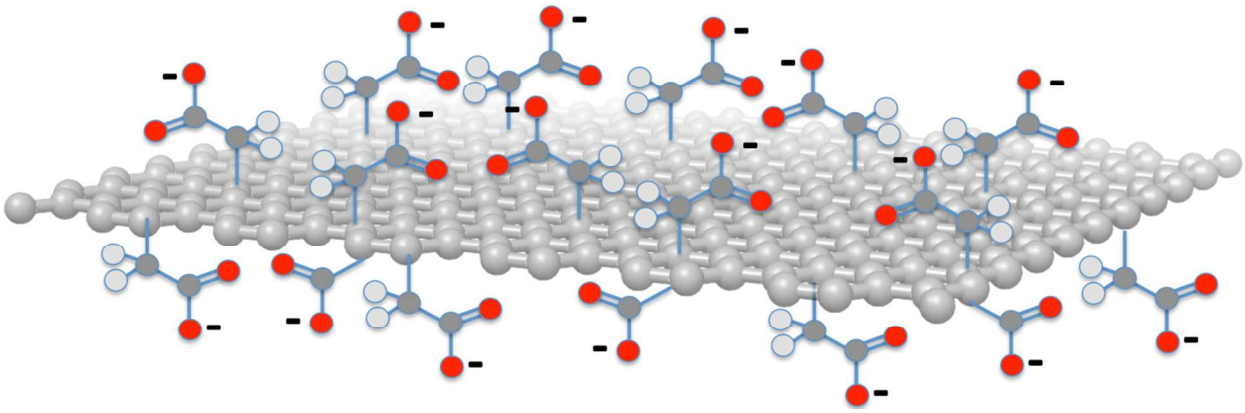

Figure 1. Schematic of CG. The graphene sheets have carbon bound acetate groups and the graphene structures may be more irregular than shown with residual oxygenated basal plane defects and oxygenated edge groups.

Interfacial Polymerization

Nanocomposites were prepared by adapting a previously described procedure for creating composites with GO [30] as shown in Figure 2.

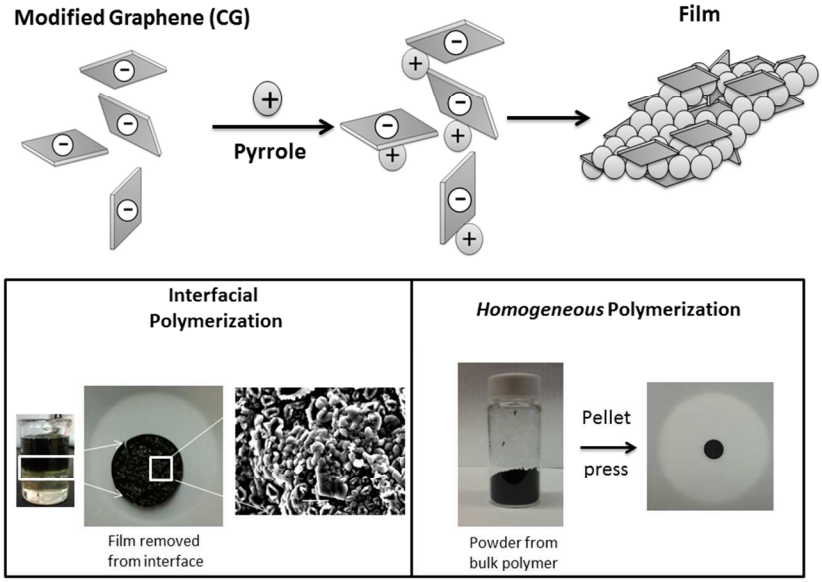

Figure 2. Scheme of interfacial/*in situ* polymerization of CG/PPy nanocomposite and synthesized samples by both methods.

Ferric chloride (300 mg) was dissolved in 15 mL of Millipore water and the resulting solution displayed pH of 2 and a zeta potential of 16.28 ± 2.43 mV. Variable amounts of CG (from 0 to 4 wt% relative to pyrrole) were introduced into these solutions and the zeta potential decreased to 6.85 ± 0.74 mV, which reflects the negative zeta potential of an aqueous solution of CG of -53.5 ± 3.67 mV. A solution of pyrrole (800 μL) in 15 mL of chloroform was added to the $FeCl_3$/CG aqueous solution in a dropwise fashion. The reaction requires the diffusion of reactants to the graphene interfaces, and the adsorption of cationic PPy on CG sheets takes place with oxidation by the ferric chloride. The solution was not agitated during the polymerization and a film grew at the water/chloroform interface over the 24 hour room temperature reaction period. This free-standing black insoluble film is easily removed and was washed with water. Circular

films of this material (1.0 cm of diameter) were used as electrodes for the creation of capacitors. These films were pre-wet with selected electrolytes before use and the sandwich-type symmetric electrodes were separated by a microporous membrane (Celgard).

In situ solution polymerization

As an alternate preparation of supercapacitor nanocomposites we investigated oxidation of pyrrole by ammonium persulfate from a stirred aqueous solution. [31-33] Variable amounts of CG (from 0 to 10% wt relative to the pyrrole amount) were dispersed in 100 mL of Millipore water with 1 hour of sonication. After dispersion of CG in water and under intense stirring at 0° C, 0.03 M of pyrrole is introduced into the aqueous solution. The pyrrole/CG solution is stirred for an additional hour and then a pre-cooled solution of ammonium persulfate (0.06 M in 50 mL of Millipore water) was added. The reaction at 0^0C is carried out under stirring over three hours. The resulting powder is filtered under vacuum and washed extensively with water. The material is dried in an oven under vacuum at 45° C for 6 hours and the resulting powder is compressed at 100 kgf/cm^2 into disc shaped pellets (1.0 cm diameter) for capacitor testing. The pellets were pre-wet with the selected electrolyte before use to create symmetric sandwich-type capacitors with each disc electrode separated by a Celgard membrane.

The morphology of thin films was analyzed by scanning electron microscopy (JSM 6060, SEM), the zeta-potential was performed using a Zeta Potential Analyzer (Zeta PALS, Brookhaven Instruments Corp) and FTIR spectra were collected by a Nexus 870 spectrometer using KBr pellets. The electrochemical responses were characterized by cyclic voltammetry (CV), charge-discharge cycling was analyzed with a potentiostat/galvanostat (Autolab PGSTAT30), and electrochemical impedance spectroscopy by the use of an impedance analyzer

(Solartron 1260/1287). Brunauer-Emmett-Teller (BET) surface area measurements were performed on a Micrometrics ASAP2020 surface area analyzer using nitrogen gas and the ASAP2020 software for analysis.

RESULTS AND DISCUSSION

FTIR analysis

FTIR spectra of pure PPy, CG and CG-PPy (1 wt% of CG/PPy) with the PPy elements prepared by interfacial and *in situ* dispersion polymerization are shown in Figures 3 and 4, respectively.

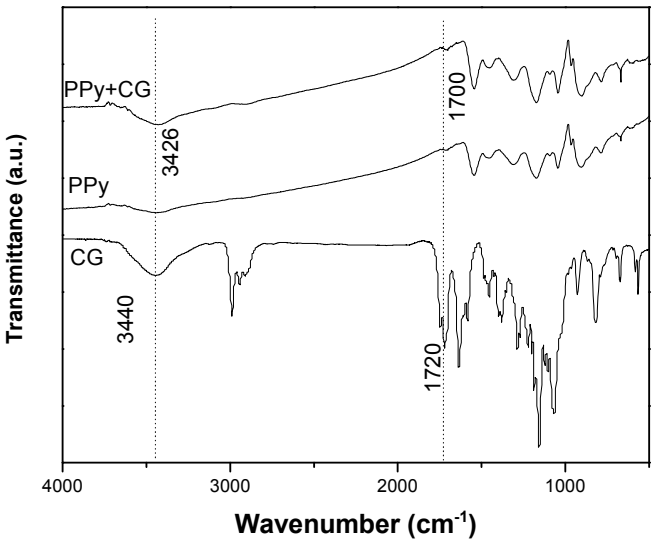

Figure 3. FTIR spectra of CG, PPy and CG/PPy (1.0 wt%) nanocomposite prepared by interfacial polymerization.

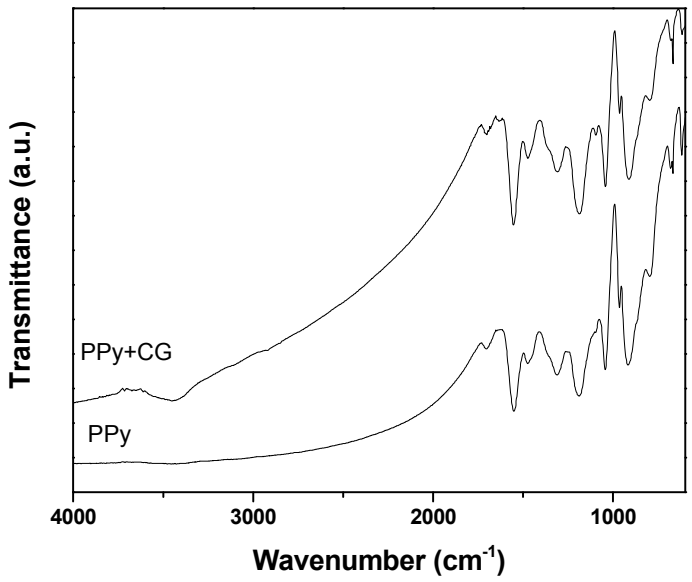

Figure 4. FTIR spectra of PPy and CG/PPy (1.0 wt%) nanocomposites prepared by *in situ* polymerization.

In the spectrum of pure polypyrrole, the absorption peaks at 3442, 1547, 1468 and 1043 cm^{-1} are assigned to the N-H, C-C, C-N stretching vibrations and C-H in plane vibrational bands of the pyrrole ring respectively, [10, 25, 30] and the peak at 1309 cm^{-1} is assigned to C-N bonds.[26] For the CG spectrum, a broad peak at 3440 cm^{-1} and peaks at 1720, 1220, 1060 cm^{-1} (Figure 3) are attributed to O-H stretching vibration, carbonyl (C=O) , C-O-C and C-O stretching vibrations, respectively. [10,24,25,27,30] In the FTIR of the nanocomposites, it is possible to identify characteristic peaks of polypyrrole (Figures 3 and 4) at 3426, 1547, 1465 cm^{-1}, in an indication that polymerization is established in the presence of CG. Some of the peaks of the nanocomposites are shifted to lower energies (as summarized in Table 1 – supporting

information), as a result of interactions between CG and PPy.[10,25,27] The CG peaks are marginally identifiable in the composite materials as a result of its low concentration.

Electrical characterization

Two different supporting electrolytes were evaluated for our nanocomposites. The response of films immersed in 1-butyl-3-methylimidazolium hexafluorophosphate and KCl aqueous solution (at different concentrations) were analyzed. These studies revealed that 1M of KCl aqueous solution provided the best capacitance and stability in devices (comparative results can be found in the supporting information). The figures of merit evaluated for our nanocomposites include the charge/discharge characteristics, the CV curves, and the impedance spectra.

In situ CG/PPy nanocomposite

The charge/discharge responses of devices (pellets of nanocomposite separated by Celgard and impregnated with 1 M of KCl aqueous solution) with a constant current of 3 mA during a complete cycle of charge and discharge are shown in Figure 5.

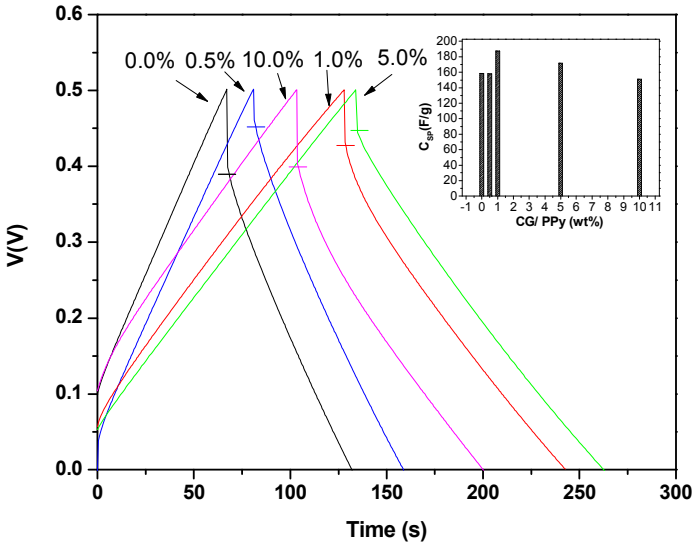

Figure 5. Galvanostatic charge/ discharge curves of CG/PPy curves (*in situ* polymerization) at different relative concentration.

The progressive inclusion of CG from 0.5 - 5.0% results in an increase in the characteristic charge/discharge times, which reflects an improvement of capacitance. Over this region we also observe a reduction in the "IR drop" in the CG/PPy composites, which is revealed in the initial rapid voltage drop in the discharge curves. This reduction reflects an increase in the conductivity with the increased CG and contributes with the improvement in the symmetry between charge and discharge curves. However, we do find that going beyond 5 wt% of CG/PPy leads to a lowering of the device performance as evidenced by the data shown for the sample containing 10 wt% CG. Notably the time per cycle is reduced and the IR drop increases. The capacitance calculated in accord with Eq. 1 is given in the inset of Figure 5 (note, the results in the inset are normalized per mass). The capacitance reaches a maximum at 1 wt% CG and progressively more CG contributes with reduction in the performance of CG/PPy devices. The improvement in the capacitance can also be detected from CV curves, as shown in Figure 6.

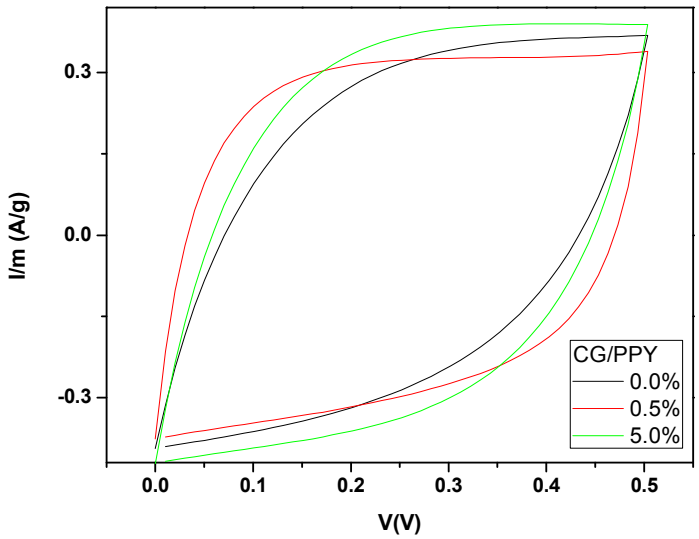

Figure 6. CV curves (at scan rate of $10mVs^{-1}$) for composites (*in situ* polymerization) with 0.0%, 0.5% and 5.0% of CG/PPy.

The inclusion of CG in the homopolymer (PPy) affects the area of curve (i.e. the capacitance) at the same time it produces a more idealized a rectangular shape, indicating that CG improves the electrical double-layer capacitance in the response of the system.[9] The dependence of capacitance with scan rate and concentration of CG is shown in Figure 7.

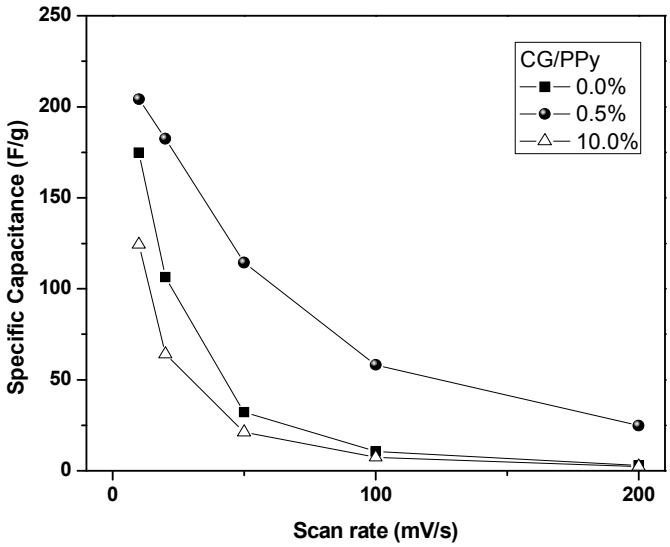

Figure 7. Capacitance of nanocomposite with 0, 0.5 and 10.0 wt% of CG/PPy (*in situ* polymerization) as a function of scan rate.

The specific capacitance of all of the samples decreases with the increase in the scan rate (as a consequence of the required time for ionic migration in the material). For all scan rates, the specific capacitance of CG/PPy (0.5 wt%) is higher than the PPy and suggests that the higher surface area of the CG composite provides improved access to the electrolyte. Analyzing the surface area by the Brunauer-Emmett-Teller (BET) method reveals a slight increase in the surface area for the 1 wt% composite, from 24.4 m^2/g for polypyrrole to 33.5 m^2/g (BET area of

the neat CG is 82 m^2/g). The other percentages show surface areas which are roughly unaltered (as summarized in Table 2 – supporting information), suggesting that superior electrical properties result from pseudocapacitance of PPy/ CG composite. Again, the inclusion of CG beyond optimal performance of device induces an overall reduction in the capacitance of device, as verified in Figure 7 for sample containing 10 wt% of CG/PPy sample.

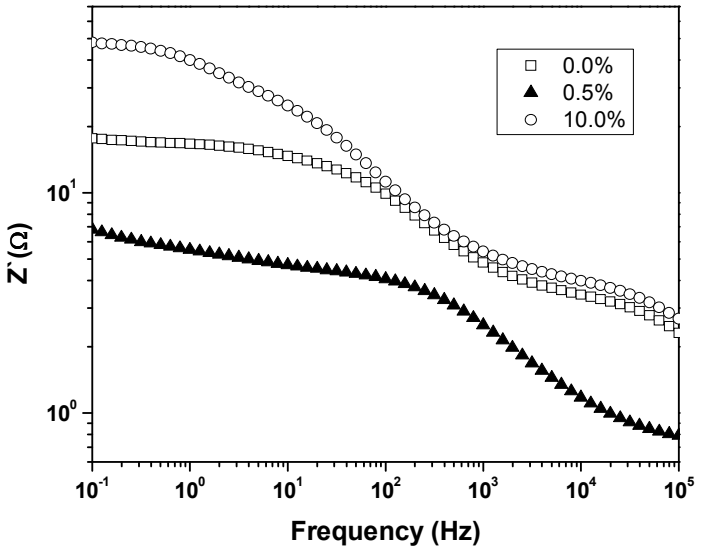

Figure 8. Spectrum of real part of impedance of samples with different relative concentration of CG/PPy (*in situ* polymerization).

To further compare the response of system CG/PPy nanocomposite with that of pure PPy we have made use of electrochemical impedance spectroscopy (Figure 8). The impedance spectrum obtained for samples containing 0 wt%, 0.5 wt% and 10.0 wt% of CG (prepared by *in situ* polymerization, using a signal amplitude of 10 mV), reveals the impedance of CG/PPy nanocomposite at a low concentration of CG is decreased, suggesting a strong interaction between PPy and CG, consistent with the changes FTIR spectrum. M. Deng *et al*. [34] state that a decrease in the impedance of PPy/GO nanocomposites can be due to the roughness induced by

graphene oxide, which manifests surface area increases. As a consequence, the charge transfer resistance and capacitance of device are improved, as verified in the galvanostatic curves. The response of devices at 10 wt% CG display elevated impedance in the free charge region (low frequency), indicating that reduction in the capacitance is a consequence of minimization in the electrical transport properties provided by the composite electrodes and reduction in the surface area. By comparison, as shown in the Table 2 – supporting information, the surface area of 10 wt% CG is reduced to 21.6 m^2/g.

CG/PPy nanocomposite by interfacial polymerization

The behavior of specific capacitance of nanocomposites prepared by interfacial polymerization is similar to the behavior observed in the devices prepared by *in situ* oxidative polymerization. The progressive inclusion of CG in the nanocomposite results in improvement of electrical properties of nanocomposite, as indicated in the Nyquist plot shown in Figure 9.

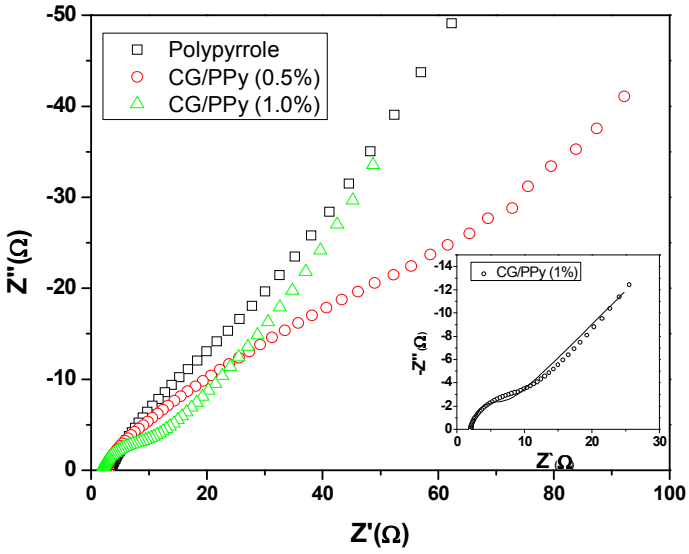

Figure 9. Nyquist plot of nanocomposite at different relative concentration of CG/PPy (interfacial polymerization).

The Nyquist plot is divided into different regions: a linear low-frequency region that characterize charge transfer to the electrode surface (electrically represented by the Warburg element) and a characteristic semicircle at high frequency. Deviations from linear response, as observed in the expanded inset of Figure 9, are attributed to the pseudocapacitance effects from the polypyrrole. In the high-frequency region, it is possible to measure the equivalent series resistance (ESR) which represents the response of electrolyte solution [9] from extrapolated intersection of the curve with real axis of impedance (Z') - corresponding to zero for Z". Other important information is relative to the knee frequency, where there is a transition from the low to high frequency response. The absence of a clear transition indicates that the resistive behavior dominates and consequently the capacitive response is minimized. As we can see in Figure 9, higher knee frequencies are obtained if compared to samples containing 0% and 1.0% of CG/PPy (interfacial polymerization), as verified for a corresponding system, as reported in the literature.[25]

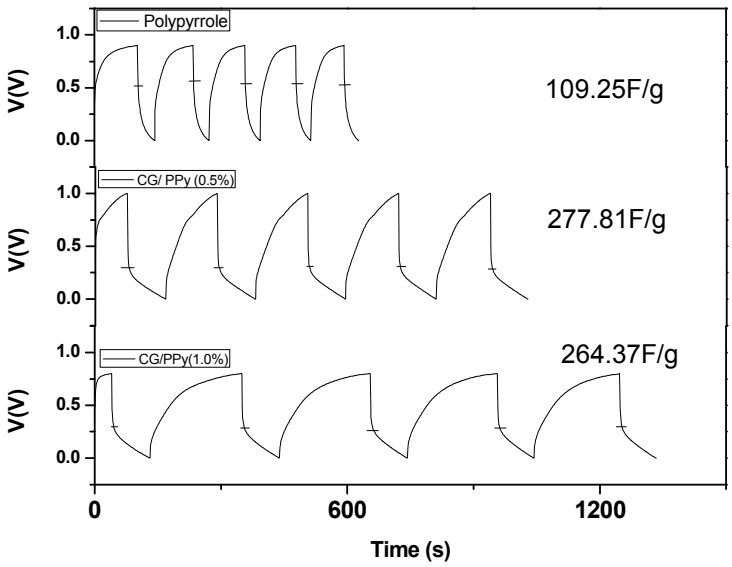

Figure 10. Charge/discharge curves of nanocomposite at different relative concentration of CG/PPy (interfacial polymerization).

In accord with the improvements in the imaginary part of impedance, the specific capacitance is enhanced with low concentrations of CG. As we can see in the charge/discharge curves of Figure 10, a reasonable improvement in the capacitance of the material is obtained with inclusion of 0.5 wt% of CG, with slight reductions at a CG concentration of 1.0 wt%. Corresponding CV curves are shown in the Fig. 11.

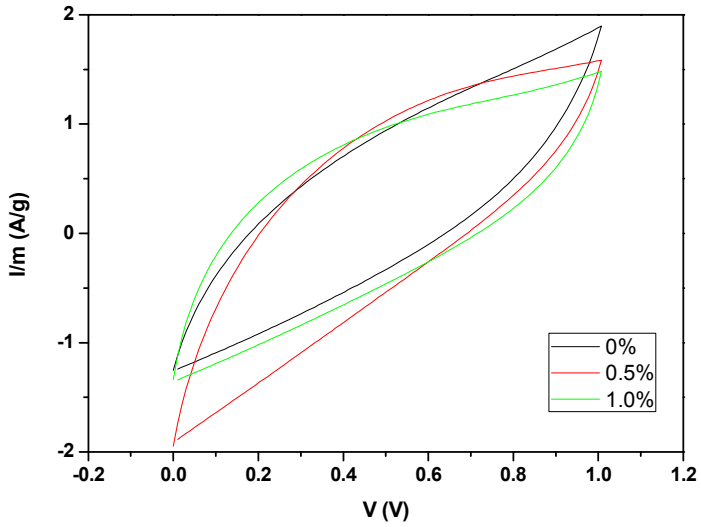

Figure 11. CV curves (at scan rate of $10mVs^{-1}$) for composites (interfacial polymerization) with 0.0%, 0.5% and 1.0% of CG/PPy.

Additionally, the BET surface area of the composites prepared by interfacial polymerization are markedly higher than those prepared by the in situ method: BET surface areas of 55.3 m^2/g and 143 m^2/g are measured for the 0.5 wt% and 1.0 wt% composites, respectively.

By comparison between two different methods of preparation, the specific capacitance of device prepared by interfacial polymerization is enhanced from 109.25 F/g determined for polypyrrole prepared under the same method to 277.81 F/g, which represents an improvement in order of > 150%. In the case of the *in situ* dispersion polymerization the capacitance of the CG/PPy composite is improved from 158.4 to 187.7 F/g, which represents an increase of 18.5%. We attribute the superior enhancements of the interfacial prepared materials to be the result of stronger interactions between PPy and CG. This analysis is consistent with the electrochemical impedance spectroscopy and is also in agreement with other composite structures reported in the literature, [35] which describe the inferior electrical performance of PPy composites with GO prepared by *in situ* homogenous polymerization to be the result of stacking of GO sheets.

An important aspect to be considered is that improvement in the specific capacitance is related with influence of CG on surface area of devices. The marginal influence of CG on the surface area of samples prepared by *in situ* polymerization provides a marginal improvement in the capacitance. However samples prepared by interfacial polymerization allow for assembly processes during the polymerization that increase the surface area and provide an improvement in specific capacitance of 150%. The direct relationship between surface area and capacitance is a consequence of an improved EDLC contribution. The higher performance of interfacial polymerization may be the result of the kinetics induced by diffusion of CG sheets to the interface, which provides an increase in the heterogeneous nucleation during polymerization and produces stronger interactions between PPy and CG.

In spite of superior properties of devices created from composites produced by interfacial polymerization, we can see that optimal concentration of CG for an optimized capacitance should be less than 1.0 wt%. The reason for this optimal concentration is likely the confluence of

a number of properties, including the carboxylate charges on the CG, the morphology induced by isolated CG sheets dispersed in the PPy, and improvement in the electrical transport.

CONCLUSION

The electrical and structural properties of nanocomposites prepared by two different methods indicate that strong interaction between polypyrrole and a modified graphene (CG) provides enhancement in the capacitance of devices. We find only small amounts of the graphene are needed in the CG/PPy composites (≈ 1 wt% CG). Two different composite preparations were examined and the interfacial preparation method provided a material with the best overall reduction in the electrical impedance, improvement in the surface area, strongest polymer-graphene interactions determined by FT-IR, and the greatest capacitance. As a result of the improvement of capacitance, synthesized materials are promising candidates for the construction of energy storage devices.

ACKNOWLEDGMENTS

This work was supported by the Brazilian Funding Agency (CNPq/Brazil) and the U.S. Army through the Institute for Soldier Nanotechnologies.

Supporting Information Available: Experimental details for the synthesis of CG, additional analysis of the FTIR spectra, Raman spectrum and BET surface areas. This material is available free of charge via the Internet at http://pubs.acs.org."

REFERENCES

(1) Dong, J.; Lin, Z. Within-day recharge of plug-in hybrid electric vehicles: Energy impact of public charging infrastructure. *Transport. Res. D-TR. E* **2012**, *17,* 405-412.

(2) Apte, S. K.; Garaje, S. N.; Valant, M. ; Kale, B. B. Eco-friendly solar light driven hydrogen production from copious waste H2S and organic dye degradation by stable and efficient orthorhombic CdS quantum dots–GeO2 glass photocatalyst. *Green Chem.* **2012**, *14*, 1455-1462.

(3) Pichierr, F. Binding of molecular hydrogen to halide anions: A computational exploration of eco-friendly materials for hydrogen storage. *Chem. Phys. Let.* **2012,** *519-520***,** 83-88.

(4) Hsieh, C.-T.; Hsu, S.-M.; Lin, J.-Y. Fabrication of Graphene-Based Electrochemical Capacitors. *Jpn. J. Appl. Phys.* **2012**, *51*, 01AH06.

(5) Zhang, J. ; Zhao, X. S. Conducting Polymers Directly Coated on Reduced Graphene Oxide Sheets as High-Performance Supercapacitor Electrodes. *J. Phys. Chem. C* **2012,** *116*, 5420-5426.

(6) Zhang, L. L.; Zhao, X. S. Carbon-based materials as supercapacitor electrodes. *Chem. Soc. Rev.* **2009**, *38*, 2520-2531.

(7) Stoller, M. D.; Ruoff, R. S. Best practice methods for determining an electrode material's performance for ultracapacitors. *Energy Environ. Sci.* **2010**, *3*, 1294-1301.

(8) Wei, L.; Sevilla, M. ; Fuertes, A. B.; Mokaya, R.; Yushin, G. Polypyrrole-Derived Activated Carbons for High-Performance Electrical Double-Layer Capacitors with Ionic Liquid Electrolyte. *Adv. Funct. Mater.* **2012,** *22*, 827-834.

(9) Liu, W.; Yan, X.; Lang, J.; Xue, Q. Effects of concentration and temperature of EMIMBF4/acetonitrile electrolyte on the supercapacitive behavior of graphene nanosheets. *J. Mater. Chem.* **2012**, *22*, 8853-8861.

(10) Si, P.; Chen, H.; Kannan, P.; Kim, D.-H. Selective and sensitive determination of dopamine by composites of polypyrrole and graphene modified electrodes. *Analyst* **2011**, *136*, 5134-5138.

(11) Paul, S.; Choi, K. S.; Lee, D. J.; Sudhagar, P.; Kang, Y. S. Factors affecting the performance of supercapacitors assembled with polypyrrole/multi-walled carbon nanotube composite electrodes. *Electrochim. Acta* **2012**, 78 649-655.

(12) Sun, Y.; Shi, G. Graphene/Polymer Composites for Energy Applications. *J. Polym. Sci. B: Polym. Phys.* **2013**, 51, 231-253.

(13) Niu , Z.; Luan , P.; Shao , Q.; Dong , H.; Li, J.; Chen , J.; Zhao , D.; Cai , L.; Zhou , W.; Chen, X.; Xie S. A "skeleton/skin" strategy for preparing ultrathin free-standing single-walled carbon nanotube/polyaniline films for high performance supercapacitor electrodes**.** *Energy Environ. Sci.* 2012 , 5, 8726-8733.

(14) Wang, J.; Xu, Y. L.; Chen, X.; Sun, X. F. Capacitance properties of single wall carbon nanotube/polypyrrole composite films. *Comp. Sci. Technol.* **2007**, *67*, 2981-2985.

(15) Khomenko, V.; Frackowiak, E.; Beguin, F. Determination of the specific capacitance of conducting polymer/nanotubes composite electrodes using different cell configurations. *Electrochim. Acta* **2005**, *50*, 2499-2506.

(16) Jang, J.; Bae, J.; Choi, M.; Yoon, S. H. Fabrication and characterization of polyaniline coated carbon nanofiber for supercapacitor. *Carbon* **2005,** *43*, 2730-2736.

(17) Liu, H.; Wang, Y.; Gou, X.; Qi, T.; Yang, J.; Ding, Y. Three-dimensional graphene/polyaniline composite material for high-performance supercapacitor applications. *Mat. Sci.Eng. B* **2013**, *178*, 293– 298.

(18) Chang, H.-H.; Chang, C.-K.; Tsai, Y.-C.; Liao, C.-S. Electrochemically synthesized graphene/polypyrrole composites and their use in supercapacitor. *Carbon* **2012**, *50,* 2331-2336.

(19) Zhao, M.-Q.; Zhang, Q.; Huang, J.-Q.; Tian, G.-L.; Chen, T.-C.; Qian, W.-Z.; Wei, F. Towards high purity graphene/single-walled carbon nanotube hybrids with improved electrochemical capacitive performance. *Carbon* **2013**, *54,* 403-411.

(20) Lee, Y.-H.; Chang, K.-H.; Hu, C.-C. Differentiate the pseudocapacitance and double-layer capacitance contributions for nitrogen-doped reduced graphene oxide in acidic and alkaline electrolytes. *J. Power Sources* **2013**, *227*, 300-308.

(21) Xiang, C., Li, M.; Zhi, M.; Manivannan, A.; Wu, N. A reduced graphene oxide/Co3O4 composite for supercapacitor electrode, J. Power Sources **2013,** *226,* 65-70.

(22) Ping, J.; Wang, Y.; Ying, Y. ; Wu, J. Application of Electrochemically Reduced Graphene Oxide on Screen-Printed Ion-Selective Electrode. *Anal. Chem.* **2012**, *84*, 3473-3479.

(23) (a) Collins, W.R.; Schmois, E.; Swager, T. M. Graphene oxide as an electrophile for carbon nucleophiles. *Chem. Commun.* **2011**, *47,* 8790-8792, (b) Collins, W. R.; Lewandowski, W.; Schmois, E.; Walish, J.; Swager, T. M. Claisen Rearrangement of Graphite Oxide: A Route to

Covalently Functionalized Graphenes. *Angew. Chem. Int. Ed. Engl.* **2011**, *50,* 8848-8852, (c) Sydlik, S. A.; Swager, T. M. Functional Graphenic Materials Via a Johnson−Claisen Rearrangement. *Adv. Funct. Mat.* In press, DOI: 10.1002/adfm.201201954.

(24) Yang, Y.; Wang, C. ; Yue, B.; Gambhir, S.; Too, C. O.; Wallace, G. G. Electrochemically Synthesized Polypyrrole/Graphene Composite Film for Lithium Batteries. *Adv. Energy Mater.* **2012**, *2,* 266-272.

(25) Zhu, C.; Zhai, J.; Wen, D.; Dong, S. Graphene oxide/polypyrrole nanocomposites: one-step electrochemical doping, coating and synergistic effect for energy storage. *J. Mater. Chem.* **2012,** *22,* 6300-6306.

(26) Basavaraja, C.; Kim, W. J.; Thinh, P.X.; Huh, D. S. Polypyrrole–Graphene Oxide Composites, Polypyrrole–Graphene Oxide Composites. *Polym. Composite.* **2011**, *32*, 2076-2083.

(27) Konwer, S.; Boruah, R.; Dolui, S. K. Studies on Conducting Polypyrrole/Graphene Oxide Composites as Supercapacitor Electrode. *J. Electron. Mater.* **2011**, *40*, 2248-2255.

(28) Pham, H. D.; Pham, V. H.; Oh, E.-S.; Chung, J. S.; Kim, S. Synthesis of polypyrrole-reduced graphene oxide composites by in-situ photopolymerization and its application as a supercapacitor electrode. *Korean J. Chem. Eng.* **2012**, *29*, 125-129.

(29) Hummers, W. S.; Offeman, R. E. Preparation of Graphitic Oxide. *J. Am. Chem. Soc.* **1958**, *80*, 1339-1339.

(30) Bora, C.; Dolui, S.K. Fabrication of polypyrrole/graphene oxide nanocomposites by liquid/liquid interfacial polymerization and evaluation of their optical, electrical and electrochemical properties. *Polymer* **2012**, *53,* 923-932.

(31) Li, L. Y.; Xia, K. Q.; Li, L.; Shang, S. M.; Guo, Q. Z.; Yang, G. P. Fabrication and characterization of free-standing polypyrrole/graphene oxide nanocomposite paper. *J. Nanop. Res.* **2012,** *14-6*, 908.

(32) Sonanave, A. C. ; Inamdar, A. I.; Dalavi, D.S.; Deshmukh, H.P.; Patil, P. S. Simple and rapid synthesis of NiO/PPy thin films with improved electrochromic performance. *Electrochim. Acta* **2010**, *55-7*, 2344-2351.

(33) Taunk, M.; Chand, S. Electrical Transport Over Wide Temperature Range In Doped And Undoped Polypyrrole. *AIP. Conf. Proc.* **2010**, 1*313,* 256-258.

(34) Deng, M.; Yang, X.; Silke, M. ; Kiu, W. M.; Xu, M.S.; Borghs, G.; Chen, H. Z. Electrochemical deposition of polypyrrole/graphene oxide composite on microelectrodes towards tuning the electrochemical properties of neural probes. *Sens. Act. B* **2011**, *158*, 176-184.

(35) Gu, Z.; Zhang, L.; Li, C. Preparation of highly conductive polypyrrole/graphite oxide composites via in situ polymerization. *J. Macromol. Sci. Part B Phys.* **2009**, *48*, 1093-1102.

TOC graphic

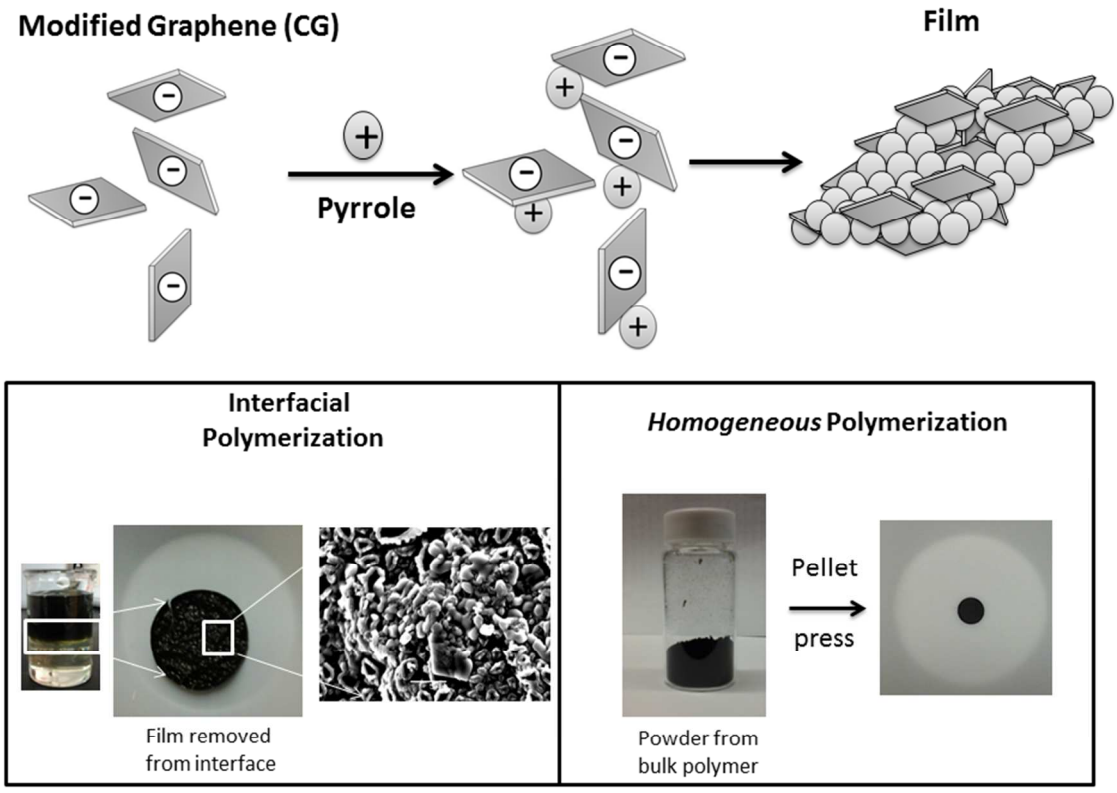

Scheme of polymerization of supercapacitors.